

Guided simulated annealing method for optimization problemsC. I. Chou,¹ R. S. Han,¹ S. P. Li,¹ and Ting-Kuo Lee^{1,2}¹*Institute of Physics, Academia Sinica, Taipei, 115 Taiwan*²*Physics Division, National Center for Theoretical Sciences, P.O. Box 2-131, Hsinchu, 300 Taiwan*

(Received 23 January 2003; revised manuscript received 28 March 2003; published 10 June 2003)

Incorporating the concept of order parameter of the mean-field theory into the simulated annealing method, we present an optimization algorithm, the guided simulated annealing method. In this method mean-field order parameters are calculated to guide the configuration search for the global minimum. Allowing fluctuations and improvement of mean-field values iteratively, this method successfully identifies global minima for several difficult optimization problems. Application of this method to the HP lattice-protein model has found another lowest-energy state for an $N=100$ sequence that was not found by other methods before. Results for spin glass models are also presented which show improvement over the previous results.

DOI: 10.1103/PhysRevE.67.066704

PACS number(s): 02.70.Tt, 87.14.Ee, 87.15.By, 87.15.Cc

I. INTRODUCTION

Optimization problems (OP's) [1] arise in areas of science, engineering, and other fields. As emphasized by Levinthal's paradox [2], the main difficulty in these OP's is the exponential increase in the search space with system size. The traveling salesman problem [3], the protein folding problem [4], and the Lennard-Jones microcluster problem [5] are some of the examples belonging to this class.

Two of the most popular numerical approaches to treat OP's are the simulated annealing (SA) method [6] and genetic algorithms [7]. For these approaches to succeed, the methods must be able to sample as much configuration space (CS) as possible. However, most of these OP's have energy landscapes filled with local minima surrounded by high barriers. Therefore many sophisticated methods were invented to avoid entrapment in local minima and to increase efficiency in configuration sampling. The local landscape paving [8], basin hopping [5], stochastic tunneling [9], the various generalized ensemble methods [10,11], or the nonextensive statistics [12] are all based on this philosophy. Even if the entrapment problem is resolved, it would not be particularly efficient to sample the multidimensional CS by random trials. It would be preferable to have some guidance about the most probable region where the global minimum is located. We will show below that the concepts used in the familiar mean-field (MF) approach in many-body problems can be useful in this regard.

In the MF approach, specific physical quantities are identified as order parameters (ORP's). These ORP's (or just one parameter) are problem specific and usually carry the most important information about the system's ground state. They acquire different values between high temperature states and the ground state. The idea of the MF approach is to use the ORP's to lead the many-body system to low-energy states so that injecting small fluctuations would bring the system to its ground state. Some understanding of the ground state is necessary to choose the correct ORP's. Fortunately, we do have information about the results we are looking for in most cases. For example, we know that Lennard-Jones clusters [5] will have most of their inner core atoms arranged with cer-

tain symmetry. The density of atoms is therefore a good ORP.

We incorporate this MF concept into the SA method. In our approach, the ORP's with some assumed initial values are used to bias the search of CS to favor the regions dictated by their values. In other words, the ORP is used as a guiding function (GF) in the search of the ground state. By changing its values iteratively, the ORP continuously adjusts its values until the ground state is reached. This combination of the SA method with a GF will be called the guided simulated annealing (GSA) method. As an illustration of the method, we will apply it to the HP lattice-protein model [11,13] and the spin glass (SG) model [14]. For the former, we have found another lowest-energy state that has not been found before for a sequence of length 100. For the latter, additional results for five-dimensional (5D) SG models are found. The method has also been successfully applied to the x-ray crystallographic problem for large molecules [15] and the Lennard-Jones cluster problem [16]. In Sec. II, we will give details of our algorithm and its implementation on the lattice HP model. Section III is the numerical result of our simulation on the lattice HP model and a further discussion of the implementation of our algorithm in optimization problems is given in Sec. IV.

II. ALGORITHM

Lattice-protein models are the simplest models that have been playing important roles in the theoretical studies of protein folding. In these models, protein chains are heteropolymers that live on two- or three-dimensional regular lattices. They are self-avoiding chains with attractive or repulsive interactions between neighboring unbonded monomers. In most simulations, people consider only two types of monomers—the hydrophobic (H) and polar (P) monomers. The reader is referred to Ref. [13] and references therein for more detailed discussion. Despite its simplicity, the number of conformations of a lattice model protein chain becomes enormous as the length of the chain grows. It is a challenging task to find the global minimum and is an ideal test for the GSA method.

Our approach begins with a population of M randomly

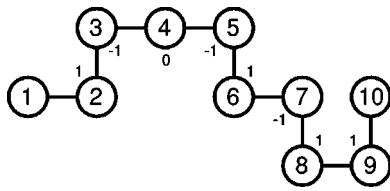


FIG. 1. A 10-monomer protein chain on a two-dimensional square lattice.

generated conformations. We let each of them evolve independently as in the usual SA method [6]. We here adopt the three commonly used Monte Carlo (MC) moves—the end move, the corner move, and the crankshaft move [11]. Aside from these moves, we also occasionally include one more type of move: a rotation of a portion of the chain about a chosen point of this chain [17]. We adopt the Metropolis rule [6] for all our MC moves. In each of the M independent runs, we keep a record of its lowest-energy solutions after a preset number of MC steps.

Our next step is to construct a GF. As mentioned above, the choice of the GF is determined by the ORP that represents an important property that is different between the low-energy and high-energy states. For a real protein, Ramachandran torsion angles are clearly good candidates for the ORP. We therefore consider the angular distribution at each monomer or more appropriately the local substructure is used as our GF. Let us consider a chain consisting of ten monomers on a two-dimensional square lattice with a conformation as shown in Fig. 1. For this protein chain, we take for each time a segment of five monomers. A total of six segments can be identified if we move along the chain from the first monomer. For each segment, we record its structure as follows. As we move along the chain, there are three different cases that we encounter: go straight (0), turn left (1), or turn right (-1). For example, for the first segment from monomer 1 to 5, we go left (1), right (-1), then straight (0).

This substructure associated with monomer 3 is denoted as $(1,-1,0)$. Let us take another example here. For the fourth segment, starting from monomer 4, we will need to make a right turn (-1), then a left turn (1), and finally a right turn (-1) in order to reach monomer 8. In this case, we use $(-1,1,-1)$ to specify its structure and this segment is associated with monomer 6. Likewise, the sixth segment, from monomer 6 to 10, can be represented by $(-1,0,1)$ and is associated with monomer 8. According to this classification, there are a total of 25 possible substructures for a segment of length 5 in two dimensions. Notice that $(1,1,1)$ and $(-1,-1,-1)$ both form closed squares and thus are not allowed.

All 25 types of substructures discussed above are for segments with five monomers and are shown in Fig. 2(a). There are, however, two segments of six monomers, shown in Fig. 2(b), which deserve special attention. Not only are they related to the crankshaft MC move, but they also seem to have special weight in the structures. Thus, if we have segments with length 6 of one of these two types $[(1,-1,-1,1)$ or $(-1,1,1,-1)]$, we will record it using these two types of substructures instead of the above 25 types. Again, these two

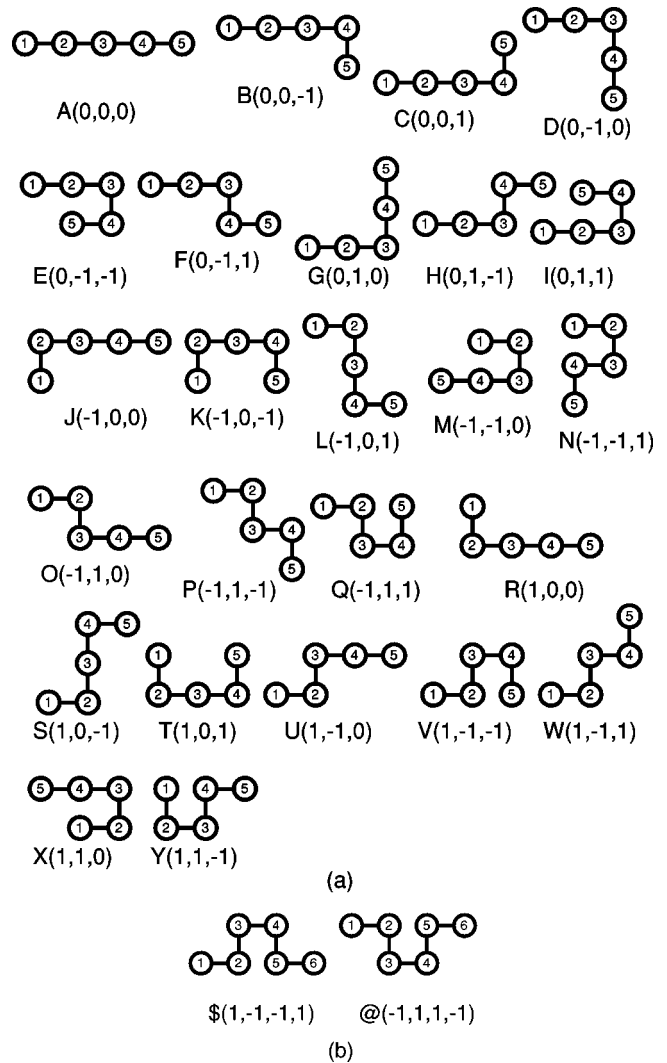


FIG. 2. (a) All 25 types of substructures of segments with length 5. (b) Two types of substructures of segments with length 6.

additional types of substructures will be associated with the third monomer of their corresponding segment [18].

We add up the number of times each substructure appears at every monomer of the chain for the M lowest-energy solutions and then make a set of distribution functions. These distribution functions, denoted by $p(i,j)$ for the j th-type substructure at the i th monomer, are our GF's for the next layer of simulation and our values of ORP's in this layer of simulation. This completes our first layer of MC simulation. In our discussion, a layer of simulation means a set of M individual SA runs for a preset MC steps plus the construction of the aforementioned GF.

There are now a total of 27 types of substructures, hence $\sum_j p(i,j) = 1$, where $1 \leq j \leq 27$. Without interaction between monomers, $p(i,j)$ is independent of monomer position i along the chain and $p(i,j) = p_0(j)$ [19].

In the second layer of simulation, a set of M independent SA runs is again performed. The GF will now be incorporated in our search. Unlike usual SA or MC rules, where every monomer has equal probability to be selected to change its substructure before the Metropolis rule is applied,

TABLE I. Evolution of GF's of each monomer for sequence 64 [17]. Only for GFs with a probability $P(l)$ larger than 33.3% are shown below.

	Largest GF in each monomer	E_{\min}
1st layer	-----N-N--Y-Y\$N--\$-----	-38
2nd layer	\$NPWP\$N@Y-N-Y\$NP\$N@Y\$N@Y\$NP\$N@Y\$N@Y\$NPWPVMKF-Y--	-39
3rd layer	-NP-P\$N@Y\$N@Y\$NP\$N@Y\$N@Y\$NP\$N@Y\$N@Y\$NPWPVMKF@Y\$NOT I	-42
4th layer	VMKFP\$N@Y\$N@Y\$NP\$N@Y\$N@Y\$NP\$N@Y\$N@Y\$NPWPVMKF@Y\$N-T I	-42

we give a higher probability to pick the substructures within the protein chain, which appear less frequent in the GF's and try to change them into substructures with a higher probability of appearance in the same set of GF's. This is very similar to what the ORP's do in the MF approach of statistical models. For example, the assumed MF magnetization in a spin model will greatly bias the direction of the spins. It should be noted that in order to allow enough fluctuations, only slightly larger weight should be given to the GF. The values of ORP's or GF will be modified when a new set of M lowest-energy states is obtained at the end of the second layer of simulation. To avoid using solutions that could already have been locally trapped, we always start the new layer simulation with M randomly generated conformations.

There are numerous ways to apply the GF in our MC process. We will here discuss a particular way chosen by us. The first step is to decide whether to take the rotational move or the three local MC moves. A small probability (about 30%) is assigned for the rotational move and the GF is only used for the three local MC moves. Before we use the local moves to change the position of a particular monomer in a certain conformation state, we first determine the monomers within the chain, which are allowed to change positions. For each of these monomers, we look for the corresponding substructure of its segment and their GF values, namely, $p(l, j)$. The probability to select which monomer is to be moved is determined by this GF value. The smaller this value is, the more likely it should be changed. Hence we define the probability to be selected proportional to $\alpha^{-p_a(l)}$, where the adjusted distribution function $p_a(l) = p(l, j) - p_0(j)$. The background distribution p_0 for the noninteracting chain is subtracted from the GF value to signify the contribution by the interaction and the sequence effect. The parameter $\alpha > 1$ is determined by tuning the efficiency of the algorithm. For end monomers, we set $p_a = 0$.

One then adds up and normalizes all the possible probabilities. The probability $P(l)$ for monomer l to be considered for a move is then

$$P(l) = \frac{\alpha^{-p_a(l)}}{\sum_m \alpha^{-p_a(m)}}, \tag{1}$$

where m is summed over all allowed monomers. Clearly if $\alpha = 1$, the GF is not used at all. If α is chosen to be much larger than 1, all the segments are forced to be equal to the largest GF values and no fluctuations are allowed. A better choice is to have α slightly larger than 1 so that the GF could

be modified during successive layers of iteration. For the data reported below, we find that it is best to have α between 1.2 and 1.3. Table I is a demonstration of the search of our algorithm in subsequent layers for sequence 64 [17].

One can see that in the first layer only a few monomers are associated with substructure GF having probabilities larger than 33.3%. The GF's with high probability of each monomer will evolve to a stable group substructure as the system evolves and the global minimum will eventually be found.

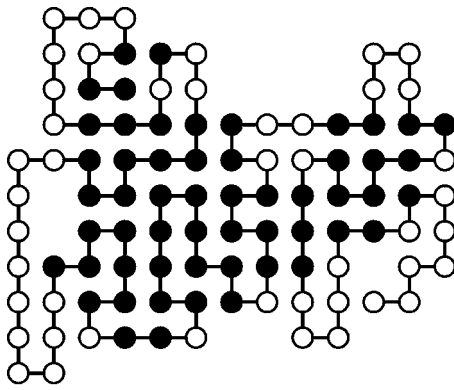
III. RESULT

Table II lists our GSA result on the 2D HP lattice model for sequences studied by many other groups. We used a population of $2N$ independent samples in each case, where N is the length of the chain. For each independent sample, we started at a certain temperature and ran for a preset number of MC steps. We then lowered the temperature and ran for the same preset number of MC steps. A set of 20 different temperatures was used. For the set of parameters we used here, a typical run on a sequence with $N = 36$ takes 46 s on a Pentium IV 1.4 GHz CPU and takes less than 10 h for the case with $N = 100$ shown in the table.

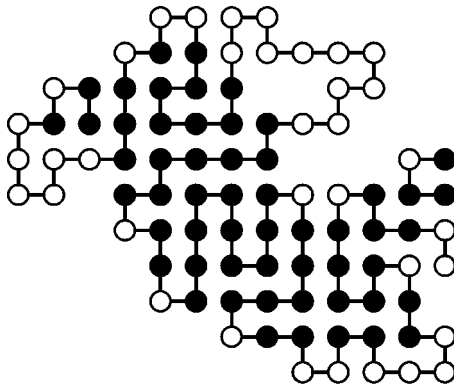
As indicated in Table II, we have been able to obtain all the previous best results of the 2D HP chains. We further obtain the lowest energy for a conformation of sequence $100_{(1)}$ that was not found by other methods. Its conformation is shown in Fig. 3(c). This is the only conformation we found with this lowest energy while more than 40 different conformations

TABLE II. Results of our algorithm on sequences of the 2D HP lattice model. "Sequence" refers to the length of the sequence. "Layers" is the number of layers in the simulation. "Steps" is the number of MC steps at each chosen temperature in each layer. "Previous" is the previous lowest-energy states using other algorithms and "Ours" is the lowest-energy states obtained by using our method.

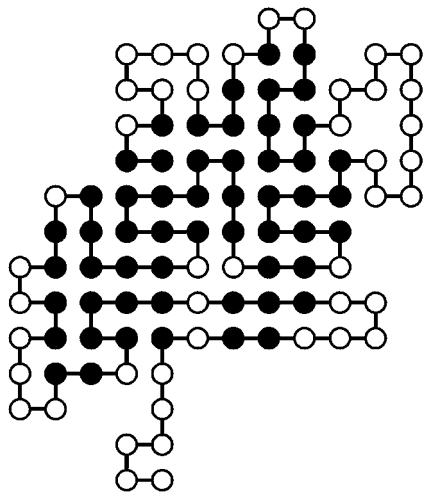
Sequence	Layers	Steps	Previous	Ours
36 [17]	2	100	-14 [17]	-14
48 [17]	2	100	-23 [20]	-23
60 [17]	2	200	-36 [23]	-36
64 [17]	4	640	-42 [21]	-42
85 [24]	2	1700	-52 [24]	-52
$100_{(1)}$ [22]	10	2000	-47 [23]	-48
$100_{(2)}$ [22]	10	2000	-50 [26]	-50



(a)



(b)

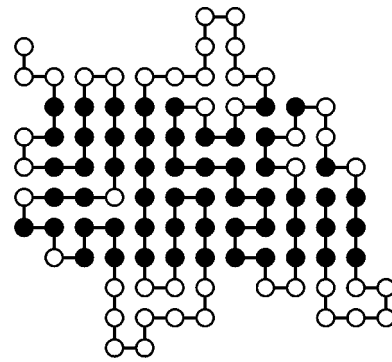


(c)

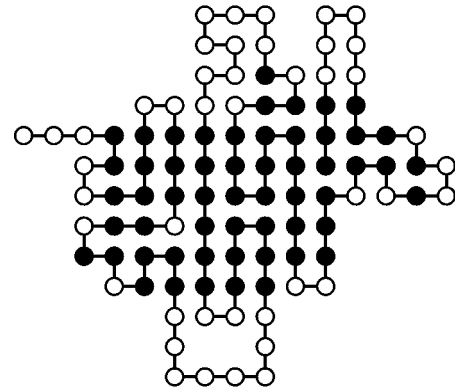
FIG. 3. Conformation of sequence 100₍₁₎. The solid dot represents the *H* monomer. There is only attractive interaction between *H* and *H* nonbonded monomers. (a) The lowest-energy conformation given in Ref. [23]. (b) The GSA result with energy $E = -47$. (c) The GSA result with lowest energy $E = -48$.

mations with energy $E = -47$ were found [one conformation is shown in Fig. 3(b)]. We have also found many conformations of sequence 100₍₂₎ with an energy $E = -50$, which are different from that given in Ref. [26] (Fig. 4), which can be provided to the reader upon request.

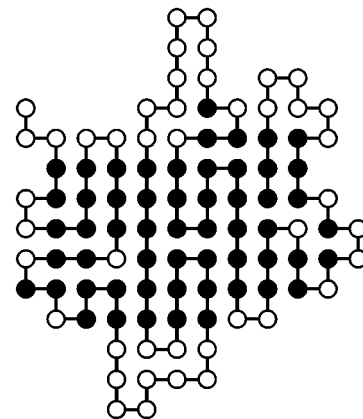
For most sequences, a few layers of iteration are enough to find the lowest energy except $N = 100$. It should be noted



(a)



(b)



(c)

FIG. 4. Conformation of sequence 100₍₂₎. The solid dot represents the *H* monomer. There is only attractive interaction between *H* and *H* nonbonded monomers. (a) The lowest-energy conformation given in Ref. [26]. (b),(c) Two GSA results with lowest energy $E = -50$.

that the number of layers and MC steps are not tuned to the optimal speed. In fact, conformations with $E = -50$ for sequence 100₍₂₎ and $E = -47$ for sequence 100₍₁₎ are found within the first seven layers already. We kept the program running to find possible lower-energy states. Since the program is very efficient, we can afford this extra search.

To understand our results better, we have carefully examined the topology of local structures in the MC simulations.

We found that local substructures form in the early stage of the search process. In addition, there is a very strong correlation between types of segments of sequence with types of substructures. For example, the *HPH* sequence segment has an unusual large probability to turn left or right at *P* monomers. *HPPH* sequence almost always has both *P* turn left or right together with both *P* likely on the surface. Their substructures are mostly related to structures shown in Fig. 2(b). Special consideration of these substructures of length 6 instead of just length 5 is important in identifying them.

To examine this further, we folded 50000 sequences of 36-mers chains to their minimal states. For a total number of 236352 *HPH* segments, 93.8% turn left or right at the middle *P* monomer, which is much larger than the average possibility 66.7%. Furthermore, most *P* monomers (89%) are found on the surfaces of the folded conformations. For the *HPPH* segment (a total of 101155), 92.6% simultaneously turn left or right at the two *P* monomers compared to the average possibility of only 22.2%. The possibility that the two *P*'s both stay on the surface is 92.5%. Since these minimal states are not necessarily the native states, we also carried out a complete search for all the native states for sequences with 11 to 17 HP monomers. Similar results are obtained. For a total of 7373 *HPH* segments, 99.5% turn left or right at the *P* monomer, and 98.8% of the *P* monomers are on the surface. For 4289 *HPPH* segments, 99.7% turn left or right at the same time at the two *P*'s. Only one *P* monomer is found in the core of the native structure.

The strong correlations observed above between a certain type of sequence segment and a particular substructure may help us locate the "native" state much faster in our approach. It should be noted that this is consistent with the recent observation by Baker [27] that simple topologies with mostly local interactions are more rapidly formed than those with nonlocal interactions. The GF or the ORP we used seem to have captured the importance of local substructures in the protein structure prediction problem.

IV. DISCUSSION

In the above, we have presented results from our simulation of the lattice HP model. The results indicate that our algorithm performs well in the search for the ground state energy and conformation of the tested protein sequences. Our algorithm can, of course, be applied to many other optimization problems. One of them is the SG problem in statistical physics. In Ref. [28], we have performed simulations in the 3D SG model [14] using our GSA method. We here performed further simulations for this model in 4D and 5D and present the results in Table III.

During the simulation, the average spin configuration at each site is kept, which is equivalent to the local magnetization, and is used as our ORP or GF for subsequent layers of simulation. The reader is referred to Ref. [28] for more detail on how to use our algorithm in SG models.

In our simulation, the number of Monte Carlo steps and layers used ranges from 300 and 2 (for $L=3$) to 1400 and 3 (for $L=7$) in the 4D case. About the same set of parameters are used in the 5D case. The CPU time for a trial run on a

TABLE III. Tests on 4D and 5D SG. L is the lattice size, m is the number of spin configuration cases, and E is the average ground state energy of the m cases. All simulations are done at $T=1.15$.

L	m	$D=4$		$D=5$	
		E	Ref. [29]	m	E
3	8000	-2.0249(7)	-2.0214(6)	5000	-2.3168(5)
4	2000	-2.0699(6)	-2.0701(4)	1000	-2.3506(4)
5	1000	-2.0849(5)	-2.0836(3)	50	-2.3530(10)
6	200	-2.0887(7)	-2.0886(6)		
7	50	-2.0904(12)	-2.0909(12)		

SUN 450 MHz processor for the 4D $L=7$ case is about 400 s. A few trial runs are performed and the best solution is chosen for each spin configuration. One can see that our result is comparable with that of Ref. [29] in the 4D case and has considerable improvement in the 5D case [30], where $E_{\infty} = -2.347(16)$.

In summary, we have presented an approach to treat general OP's with continuous or discrete variables. Based on the idea of the MF theory, the GSA method introduces ORP's. These ORP's are then used as a GF to help direct the search of global minimum in the MC process. The method is illustrated by applying to the HP lattice-protein model. We have found all the putative ground state energies reported for the chains that we tested. One more ground state for a particular sequence of length 100 has been found. In addition, strong correlations between particular sequence segments and substructures are found. We have also discussed briefly the method in the SG problem. The results of the 4D and 5D spin glass models are also given here. As discussed in Ref. [28], the present algorithm has clear superiority over the conventional simulated annealing method. In Ref. [28], the algorithm was applied to the traveling salesman problem. As a comparison, a simulation was performed on the d198 case using the conventional simulated annealing method with 2-opt moves, for 100 trial runs with 45000 Monte Carlo steps per run. The average value for the best solution of the 100 trial runs is 1.07% above the optimal value and the best solution is 15843 while 23 out of 100 trial runs could locate the optimal solution (15780) using our algorithm with an equivalent number of Monte Carlo steps.

This GSA method has several special features. It emphasizes biased search in CS for the global minimum instead of the nonbiased search algorithm used by most other approaches [1]. This bias is guided by introducing the ORP for the OP. Depending on the nature of the particular OP, the ORP or the GF must be selected differently. Besides the cost function or the energy function, other important properties of the problem are included by ORP. As one can conceive, using the GF's in the algorithm will give more guidance to the optimum search and one will obtain improvement in most cases. This is indeed the case when we try different GFs in some of the optimization problems.

Because of the constraint of the ORP or GF, the CS to be searched is greatly reduced as the system gets to lower and lower energy. Thus less computing time is used in our method.

- [1] R. Horst and P.M. Pardalos, *Handbook of Global Optimization* (Kluwer Academic, Dordrecht, 1995).
- [2] C. Levinthal, in *Mössbauer Spectroscopy in Biological Systems*, Proceedings of a Meeting Held at Allerton House, edited by J.T.P. DeBrunner and E. Munck (University of Illinois Press, Champaign, 1969), p. 22.
- [3] G. Reinelt, *The Travelling Salesman: Computational Solutions for the TSP Applications* (Springer-Verlag, Berlin, 1994).
- [4] See, e.g., *Protein Folding*, edited by T.E. Creighton (Freeman, New York, 1992).
- [5] D.J. Wales, J.P.K. Doye, A. Dullweber, and F.Y. Naumkin, The Cambridge Cluster Database, URL <http://brian.ch.cam.ac.uk/CCD.html>
- [6] S. Kirkpatrick, C.D. Gelatt, Jr., and M.P. Vecchi, *Science* (Washington, DC, U.S.) **220**, 671 (1983); N. Metropolis, A. Rosenbluth, M. Rosenbluth, A. Teller, and E. Teller, *J. Chem. Phys.* **21**, 1087 (1953).
- [7] See, e.g., D.E. Goldberg, *Genetic Algorithms in Search, Optimization and Machine Learning* (Addison-Wesley, Reading, 1989).
- [8] U.H.E. Hansmann and L.T. Wille, *Phys. Rev. Lett.* **88**, 68105 (2002).
- [9] W. Wenzel and K. Hamacher, *Phys. Rev. Lett.* **82**, 3003 (1999).
- [10] B.A. Berg and T. Neuhaus, *Phys. Lett. B* **267**, 249 (1991).
- [11] U.H.E. Hansmann and Y. Okamoto, *Annual Reviews of Computational Physics*, edited by D. Stauffer (World Scientific, Singapore, 1999), Vol. VI, p. 129.
- [12] C. Tsallis, *J. Stat. Phys.* **52**, 479 (1998).
- [13] H.S. Chan, H. Kaya, and S. Shimizu, in *Current Topics in Computational Biology*, edited by T. Jiang *et al.* (MIT Press, Cambridge, 2002).
- [14] S.F. Edwards and P.W. Anderson, *J. Phys. F: Met. Phys.* **5**, 965 (1975).
- [15] C.I. Chou and T.K. Lee, *Acta Crystallogr., Sect. A: Found. Crystallogr.* **A58**, 42 (2001).
- [16] C.I. Chou and T.K. Lee (unpublished).
- [17] R. Unger and J. Moult, *J. Mol. Biol.* **231**, 75 (1993).
- [18] For a protein chain of length N , there are only $N-4$ segments since the first two monomers at each end do not have segments to be associated with.
- [19] For substructures $(1,1,0)$, $(1,1,-1)$, $(-1,-1,0)$, and $(-1,-1,1)$, $p_0=1/18$; $(1,-1,-1,1)$, $(1,-1,-1,0)$, $(-1,1,1,-1)$, and $(-1,1,1,0)$, $p_0=1/54$; and $p_0=1/27$ for all the remaining 19 types.
- [20] L. Toma and S. Toma, *Protein Sci.* **5**, 147 (1996).
- [21] T.C. Beutler and K.A. Dill, *Protein Sci.* **5**, 2037 (1996).
- [22] R. Ramakrishnan, B. Ramachandran, and J.F. Pekny, *J. Chem. Phys.* **106**, 2418 (1996).
- [23] H. Frauenkron, U. Bastolla, E. Gerstner, P. Grassberger, and W. Nadler, *Phys. Rev. Lett.* **80**, 3149 (1998).
- [24] F. Liang and W.H. Wong, *J. Chem. Phys.* **115**, 3374 (2001).
- [25] Ugo Bastolla, Helge Frauenkron, Erwin Gerstner, Peter Grassberger, and Walter Nadler, *Proteins: Struct., Funct., Genet.* **32**, 52 (1998).
- [26] G. Chikenji, M. Kikuchi, and Y. Iba, *Phys. Rev. Lett.* **83**, 1886 (1999).
- [27] David Baker, *Nature (London)* **405**, 39 (2000).
- [28] S.P. Li, *Int. J. Mod. Phys. C* **13**, 1365 (2002).
- [29] S. Boettcher and A.G. Percus, *Phys. Rev. Lett.* **86**, 5211 (2001).
- [30] T. Wanschura, D.A. Coley, and S. Migowsky, *Solid State Commun.* **99**, 247 (1996).